# *IET Renewable Power Generation*

## Special Issue Call for Papers

**Be Seen. Be Cited.**
**Submit your work to a new IET special issue**

Connect with researchers and experts in your field and share knowledge.

Be part of the latest research trends, faster.

**Read more**

The Institution of Engineering and Technology

Check for updates

Received: 8 March 2021 | Revised: 31 May 2021 | Accepted: 23 July 2021

DOI: 10.1049/rpg2.12268

IET Renewable Power Generation

The Institution of Engineering and Technology WILEY

ORIGINAL RESEARCH PAPER

# Modular horizontal pendulum wave energy converter: Exploring feasibility to power ocean observation applications in the U.S. pacific northwest

**Chris Dizon**[1] | **Robert J. Cavagnaro**[2] | **Bryson Robertson**[3] | **Ted K. Brekken**[1]

[1] Electrical and Computer Engineering, Oregon State University, Corvallis, Oregon, USA

[2] Pacific Northwest National Laboratory, Sequim, Washington, USA

[3] Civil and Construction Engineering, Oregon State University, Corvallis, Oregon, USA

**Correspondence**
Chris Dizon, Electrical and Computer Engineering, Oregon State University, Corvallis, Oregon, USA.
Email: dizonc@oregonstate.edu

**Funding information**
Oak Ridge Institute for Science and Education, Grant/Award Number: DOE-EERE-RPP-WPTO-2019-3001

**Abstract**

Marine renewable energy as a power source for ocean observation applications has the potential to allow longer deployment operations due to the consistent, higher, and denser energy available from this resource. This additionally could encourage deployments in remote locations where maintenance is costly or resource availability is low if dependent on solar power. More importantly, gaps in spatial data could be filled. This paper examines the feasibility of a modular horizontal pendulum wave energy converter to power National Data Buoy Center's Self-Contained Ocean Observations Payload (SCOOP) off the coast of Washington State, U.S. The effect on power output was studied when the pendulum's radius arm, mass, and power take-off damping were varied. Results using Matlab toolbox WEC-Sim revealed positive correlation between radius arm length and mass to power output, where power maximised for optimal damping values. Seasonal trends in power were not significant, where a 20 kg pendulum mass was needed to meet the SCOOP base power requirement of 5 W throughout the year.

## 1 | INTRODUCTION

The desire to explore how marine applications could benefit from marine renewable energy (MRE) has increased in recent years due to the advantages this energy source could provide compared to traditional methods (e.g. battery or solar), including consistent, higher year-round power, and the predictable nature of the resource. The Department of Energy's (DOE) Water Power Technology Office (WPTO) has been leading this front under the Powering The Blue Economy Initiative to identify at-sea or remote coastal community applications where MRE could provide a different means to meet power requirements while providing these additional benefits [1]. Both the National Renewable Energy Laboratory (NREL) and the Pacific Northwest National Laboratory (PNNL) formulated the results in the report, providing background information and a value proposition for MRE integration with eight unique markets. Subsequently, both national laboratories conducted a large outreach effort to various stakeholders within the ocean observation sector of the blue economy, with a main takeaway being power limitations are a consistent issue across many applications [2, 3].

While MRE could prove to be an answer to these gaps, the question still remains on how to integrate mechanisms harvesting energy from the ocean and the end-use application. A core challenge to realising MRE-powered blue economy applications is the nascent state of MRE technology compared to other renewable sources, with many knowledge gaps such as the optimal design topology, control methods, or power take-off (PTO) systems. This is evident by the numerous operating principles a MRE design could function by. Those specific to the focus of this paper, wave energy converters (WEC), include oscillating water columns (e.g. Ocean Energy), attenuators (e.g. Pelamis), point absorbers (e.g. PowerBuoy), oscillating surge converters (e.g. Oyster), and rotating mass (e.g. Wello Penguin) operation types [4]. Additionally, all these utilise different PTOs in the form of hydraulics, air turbines, hydro turbines, or direct mechanical or electrical drive systems to convert the energy from the waves into electricity. Although there are various ways to design a WEC, the common goal remains the

This is an open access article under the terms of the Creative Commons Attribution License, which permits use, distribution and reproduction in any medium, provided the original work is properly cited.
© 2021 The Authors. *IET Renewable Power Generation* published by John Wiley & Sons Ltd on behalf of The Institution of Engineering and Technology

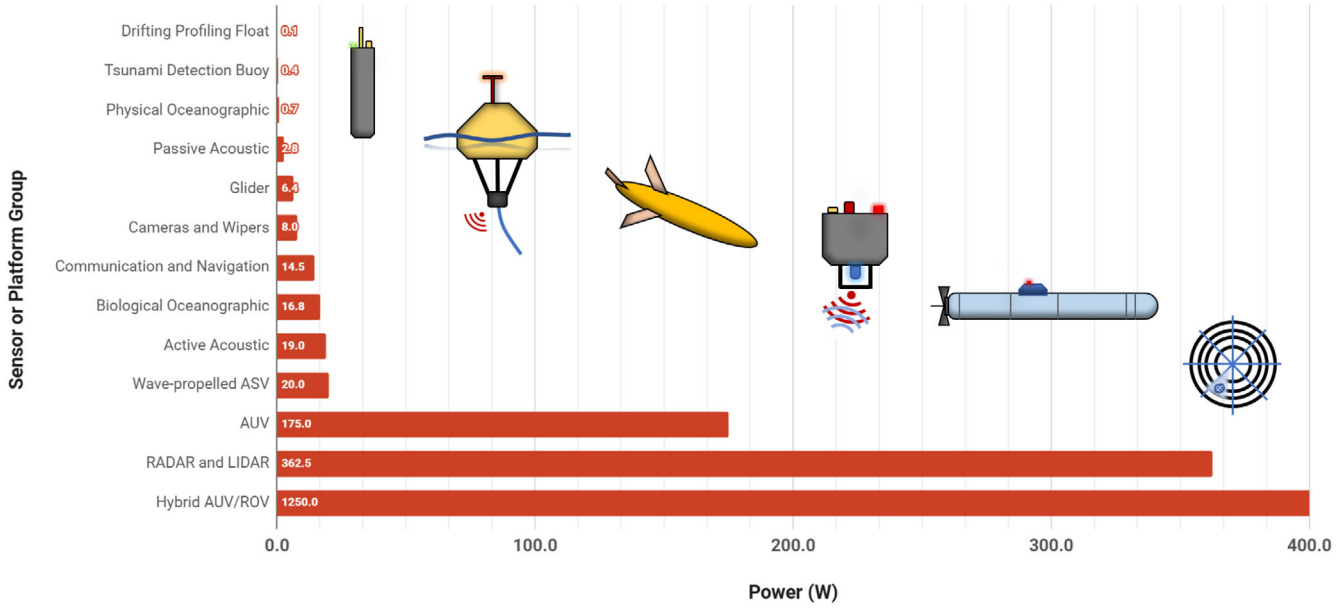


**FIGURE 1** Average power requirements of ocean observation sensors and platforms. Abbreviations: ASV (autonomous surface vehicle), AUV (autonomous underwater vehicle), ROV (remotely operated vehicle). The SCOOP requirement of 5.0 to 16.5 W is within range of similar oceanographic sensors [2]

same; to determine which topology produces the most power given environmental conditions. The large focus of this goal has been developing such devices that can supply power to the electric grid, however as the motivation behind the DOE report, there is large potential for marine applications to benefit from being powered by MRE. This effort in research has just begun, noted by multiple marine energy companies receiving grants on co-development of marine energy at smaller scales in 2020 from the WPTO [5], looking to further investigate the questions of coupling MRE to marine applications. The next essential step, then, is exploring specific WEC designs and their ability to meet applications power requirements.

This paper examines coupling a modular horizontal pendulum wave energy converter (HPWEC) to an application in the blue economy and its feasibility to power this application. Detailed analysis will cover the effect PTO damping, pendulum mass, and length of the pendulum radius arm values have on its power output capabilities. Performance is benchmarked against the requirements of a specific marine application: powering coastal weather buoys measuring ocean and atmospheric properties.

## 2 | APPLICATION CASE STUDY

A detailed application case study analysing the feasibility of powering weather buoy systems using a modular HPWEC, (i.e. the WEC is directly connected/integrated onto the buoy as a distinct device) is presented. The following subsections describe aspects of the case study in detail including the power range, site location, design of the weather buoy, community responses, and additional features considered for simulation such as mooring and data range.

### 2.1 | Power range

The power range of interest is based on the requirements of the self-contained ocean observations payload (SCOOP) system found on the National Oceanic and Atmospheric Administration (NOAA) National Data Buoy Center's (NDBC) weather buoys. SCOOP and similar meteorological and oceanographic sensor buoys host a variety of sensors reporting values such as wave height and period, wind speed, and direction, sea temperature, and air pressure which are used to understand and predict conditions and changes in the weather, climate, and ocean environment [6]. Typical power consumption ranges between a baseline of 5 W and peak of 16.5 W during periodic data transmission bursts [3], which are the basis for evaluating simulation power outputs in the results section. It is noted that this also falls within the average power requirements shown in Figure 1 for oceanographic sensors and communications equipment [2].

### 2.2 | Location of interest

The study will be applied to NDBC Station 46041 located 45 nautical miles northwest of Aberdeen, WA, U.S. in a water depth of 128 m [6]. This site was chosen for two desirable characteristics. First, the weather buoy at this station hosts the instrumentation payload modeled in our case study. Compared to more power-intensive ocean observing platforms or applications (Figure 1), these power requirements are generally in the lower range, providing a low bound to determining what power needs the modular HPWEC can meet. Second, the location of the buoy is in the Pacific Northwest of the United States which is known to have a large wave energy resource [7, 8] making it an ideal location for the integrated system to be operating in.

17521424, 2021, 14, Downloaded from https://ietresearch.onlinelibrary.wiley.com/doi/10.1049/rpg2.12268 by Battelle Memorial Institute, Wiley Online Library on [29/06/2023]. See the Terms and Conditions (https://onlinelibrary.wiley.com/terms-and-conditions) on Wiley Online Library for rules of use; OA articles are governed by the applicable Creative Commons License

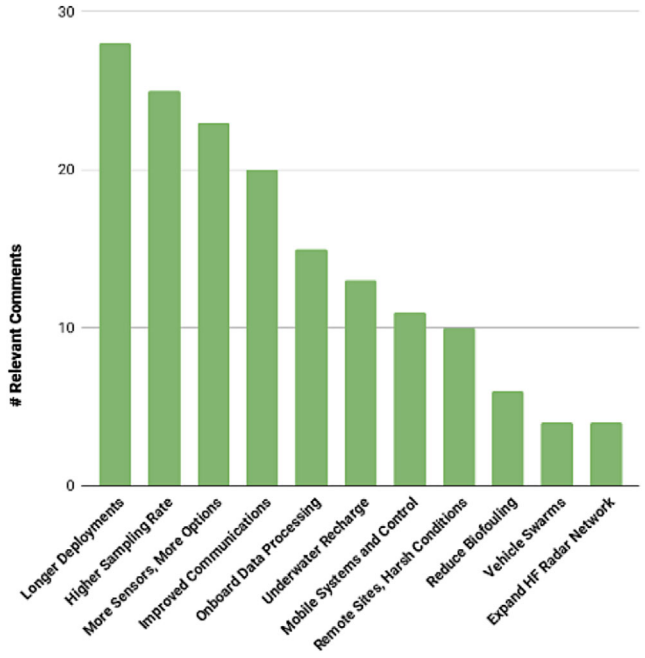


**FIGURE 2** End-user priorities for uses of additional power for ocean observing applications; most occurring theme being longer deployments [2]

An additional note to mention is operation in remote coastal areas, a theme recorded from ocean application users in a survey showing responses on possibilities if more power were available (Figure 2) [2]. The location of Station 46041 is situated along the coast of Washington State where infrastructure is limited equating to increased costs to maintain and operate systems due to difficulty of access. Typical maintenance intervals of these buoys are 12 to 18 months to keep sensors operational [3]. Currently, the buoy is powered by solar panels [2, 9], however operations in the ocean environment leads to salt accumulation which can impact their lifetime and efficiency [10]. The dependence on solar has the potential to limit the amount of power provided which additionally has an affect on the location and duration of the operation, leading to decrease use in remote areas and gaps in spatial data such as locations located closer to the poles where the solar resource availability is limited [3].

Combining a HPWEC with the buoy could lead to a longer operating period, the main desire noted by ocean application users (Figure 2), as well as removing the need for routine annual check-ins and opening up the possibility of different operating locations. As to how the design of the HPWEC accomplishes this is described later in its respective section.

## 2.3 | Coastal weather buoy modelling

A buoy like the one used for NDBC Station 46041 can be divided into two main components: the hull and the instrument payload. The hull is an AXYS 3 m discus buoy (3 m buoy) [9, 11] whose dimensions and weight of each separate structure were available after discussions with AXYS technologies (A. Velasco, personal communication, February 15 2021). Information

**TABLE 1** Mass property and dimension values for system components

| Type | Mass [kg] | COG | Diameter [m] |
|---|---|---|---|
| 3 m buoy | 1500 | [0,0,−0.03] | 1.7 |
| SCOOP | 90 | [0,0,1.7] | 0.3 |
| HPWEC housing | 10 | [−0.48,−0.64,0.50] | 0.6 |
| Pendulum | 14-100 | [−0.37,−0.54,0.52] | 0.4 |

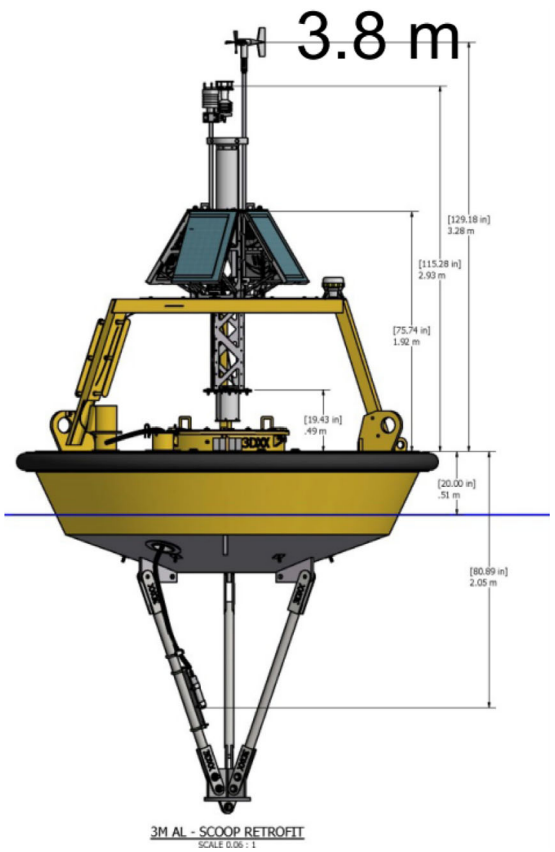


**FIGURE 3** NDBC buoy with SCOOP payload [11]

specific to the SCOOP payload was found through NDBC public presentations and research articles [11, 12]. This led to knowledge of the overall waterline, dimensions, and weight of the integrated AXYS 3 m-discus SCOOP buoy. Physical modelling was done in SolidWorks [13] to obtain mass properties such as moment of inertia (MOI) and center of gravity (COG) after applying the information from the aforementioned sources. To acquire the hydrodynamic response of the buoy in various sea states, it was then simulated in Ansys AQWA [14] using the aforementioned information to generate the hydrodynamic files of the coastal buoy. This software simulates the system through a range of frequencies and outputs responses for each frequency such as the added mass, radiation damping, Froude–Krylov, Diffraction, and response amplitude operators. Both solid modeling and hydrodynamic output files are used during power simulations described in Section 6. General dimensions and estimated mass properties of the 3 m buoy and the SCOOP payload are reported in Table 1 and Figure 3.

17521424, 2021, 14, Downloaded from https://ietresearch.onlinelibrary.wiley.com/doi/10.1049/rpg2.12268 by Battelle Memorial Institute, Wiley Online Library on [29/06/2023]. See the Terms and Conditions (https://onlinelibrary.wiley.com/terms-and-conditions) on Wiley Online Library for rules of use; OA articles are governed by the applicable Creative Commons License

## 2.4 | Mooring

Mooring systems used by NDBC can consist of a combination of chain, wire, nylon, and other polypropylene materials depending on the depth and buoy dimensions [15, 16]. Specifically, single-point surface moorings have been used by NDBC for their 3 m buoys and an all-chain mooring setup for depths up to 90 m and semi-taut for depths between 60 to 600 m [16]. To stay within the main focus of the paper, chain is used to represent the entirety of a simplified mooring system. During simulation, the library MoorDyn was used to include mooring into the simulation [17]. Values needed to run this were vessel and fixed locations of the mooring, its material, diameter, axial stiffness, weight, and unstretched length. The vessel and fixed locations are known from the AXYS schematics and the depth of the water, and the type of mooring has been chosen as chain. The axial stiffness of the chain can be calculated using elongation properties provided by the manufacturer [18]:

$$E = (5.40 - 4\,d) \times 10^{10} \tag{1}$$

$$A = \frac{2\pi d^2}{4} \tag{2}$$

where $E$ [N/m$^2$] is the elastic modulus, $A$ [m$^2$] is the chain area, and $d$ [m] is the chain diameter. The area is multiplied by two to account for the cross sectional area of two bars. The axial stiffness, $EA$ is $E$ multiplied by $A$. A 10 to 45 mm diameter chain is used in depths 2 to 150 m with a mooring scope (ratio of chain length to water depth) between 1.5 to 4.0 [19]. For JEYCO Studless Chain Grade 3 25 mm diameter chain, $EA = 5.2 \times 10^7$ N and the weight of this chain is 12.63 kg/m [18]. For a depth of 128 m with a mooring scope of 2, the unstretched length is then 256 m.

## 2.5 | Data range

To understand seasonal variation of the power output of the HPWEC, simulations were performed for each season of the year, defined as follows: Fall—September, October, November; Winter—December, January, February; Spring—March, April, May; Summer—June, July, August. NDBC's yearly data from each buoy station are publicly available. The year 2019 was chosen due to it having the most recent data with the least amount of missing values.

# 3 | HPWEC MODELLING

## 3.1 | Overview of design

The pendulum-PTO design is straightforward and has been shown to operate well in both small and large sea states [20]. The basic components and assembly of this design are shown in Figure 4. When developed appropriately, such designs require a minimum amount of mechanical parts, possibly eliminating the need for gearboxes or complex control techniques [21]. The concept is that rotation of a pendulum attached to a gear-and-pinion system drives an electrical generator. To charge a battery, an AC–DC converter is required, where a properly designed system will have a combined approximate efficiency of 90%. Additionally, the round trip efficiency of a lithium-ion battery is around 86% [22], leading to a total efficiency of 77.4%.

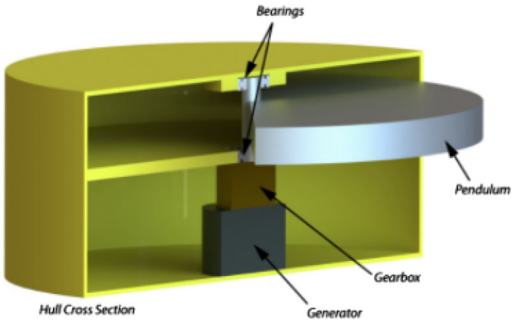


**FIGURE 4** Basic components and assembly of a HPWEC [20]; pendulum rotates to drive electrical generator

The HPWEC design offers the advantage of a completely enclosed system that is not subject to the ocean's harsh environment, therefore increasing longevity whereas other PTO methods' lifespans are cut short due to corrosion or features used to mitigate corrosion failing early. An example of such would be the linear generator point absorber, where principal components such as the stator, translator, and heaving buoy are generally exposed to salty conditions. While various sealing approaches can be used to protect sensitive components on such a point absorber, a dynamic seal separating a dry housing from a rotating or oscillating component exposed to the elements is likely required. Reducing friction and heating in dynamic seals becomes an engineering challenge with failure creating the potential to shorten the system's lifespan. This again speaks well to the fact that the pendulum's design depends on an internal moving system. Also, due to the fact that these components are within an enclosed system, all major assembly takes place onshore as opposed to offshore making deployment and recovery easier. When using a modular version of it, this gives the user the ability to produce power for their application simply by loading the device onto their pre-existing platform where it operates with the motion to the waves. Electrical integration may be as simple as connecting a single power cord to the end-user system. The modular nature of the device also provides the advantage of not being limited to one application or requiring an additional separate mooring system as it can operate directly on the platform. This additionally allows convenient maintenance of the WEC as it is its own distinct device not integrated into the system, such as the design proposed by Triton Systems [5, 23]. This would allow removal of the device for maintenance on the vessel or on land as opposed to working on the buoy or removing the buoy itself, increasing cost. This makes the pendulum design ideal for remote locations, where maintenance is costly and potentially dangerous.

17521424, 2021, 14, Downloaded from https://ietresearch.onlinelibrary.wiley.com/doi/10.1049/rpg2.12268 by Battelle Memorial Institute, Wiley Online Library on [29/06/2023]. See the Terms and Conditions (https://onlinelibrary.wiley.com/terms-and-conditions) on Wiley Online Library for rules of use; OA articles are governed by the applicable Creative Commons License

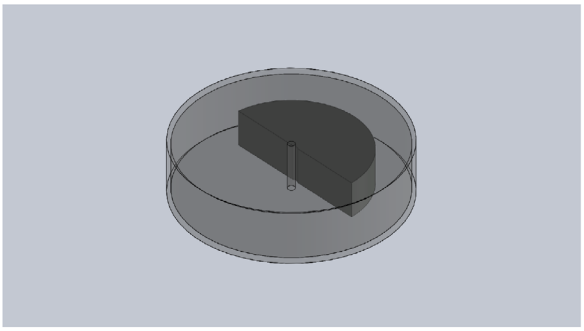

**FIGURE 5** Isometric transparent view of HPWEC cylinder housing with half moon pendulum

Since the advantage of the pendulum-PTO compared to other PTO designs is its robustness and longevity, this would pair well with systems deployed for long periods of time (years) and in remote locations where maintenance and routine check-ups are not practical options such as the case study location. Referencing the results of stakeholder surveys (Figure 2) again, the theme with the highest amount of relevant comments was 'longer deployments" which aligns well with the HPWECs design and also with the possibility of operating in "remote sites, and harsh conditions" [2]. Additionally, most rechargeable systems utilise solar PV panels, but in the Pacific Northwest, solar (compared to wave energy) is not amply available year-round nor is it the most concentrated energy source, requiring more panels and therefore space to equate to the energy available in waves [7]. With more power available, better quality sensors that require higher power, but less calibration and maintenance, may become viable as well. The above items represent an opportunity to study the feasibility of utilising a HPWEC to power such systems.

### 3.2 | Modular system

This subsection details the basic shape of the modular HPWEC for the application case study. The design is based on a simple empty cylinder shape that houses the pendulum-PTO. The housing radius is 0.3 m and height 0.18 m with a thickness of 0.01 m. The pendulum design considered was a half moon shape of radius 0.2 m and height 0.15 m. The radius arm length is the distance from the HPWEC central axis to the pendulum COG which will be varied in simulation to study the effect it has on power output. The modular HPWEC is shown in Figure 5. Dimensions were based on designing the smallest pendulum size with the ability to be physically manufactured within the mass ranges considered (14 to 100 kg) and to be as close as possible to the center of a 3 m buoy. Additionally, dimension and location decisions were chosen to mitigate as much as possible the effects of the pendulum's motion on the buoy's original hydrodynamics.

Hypothetical volume and mass limits for modular devices on NDBC 3 m buoys were obtained from NOAA of 0.06 $m^3$ and 14 kg, respectively. The volume of the studied modular HPWEC is 0.02 $m^3$ and HPWEC weights used during simulations that met the SCOOP power requirement will be compared to the 14 kg limit to examine if this restriction can be met. The model of the integrated system is shown in Figure 6. General dimensions of the HPWEC housing and pendulum are in Table 1, noting that the values are taken from its location on the buoy with a radius arm length of 0.18 m.

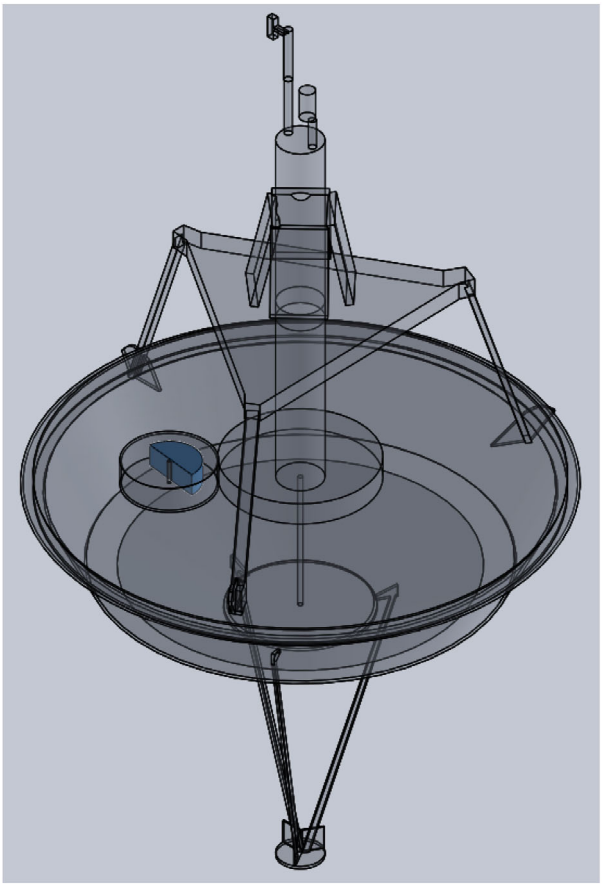

**FIGURE 6** Isometric transparent view of the integrated system; pendulum highlighted in blue, HPWEC housing rigidly connected to 3 m buoy

## 4 | RESOURCE ASSESSMENT: QUANTIFYING THE WAVE CLIMATE

To generate power outputs from the integrated system, the sea state it will be simulated through needs to be calculated. A resource assessment is used to determine the distribution of significant wave height ($H_s$) and peak period ($T_p$) during year 2019 at NDBC Station 46041. These will help define the most frequently occurring sea states and necessary parameters for developing an irregular sea state realisation using the Bretschneider spectrum to be used in power simulations.

### 4.1 | Bivariate histograms

When representing an irregular sea state, the parameters needed ($H_s$ and $T_p$) are based on a bivariate histogram; a representation

17521424, 2021, 14, Downloaded from https://ietresearch.onlinelibrary.wiley.com/doi/10.1049/rpg2.12268 by Battelle Memorial Institute, Wiley Online Library on [29/06/2023]. See the Terms and Conditions (https://onlinelibrary.wiley.com/terms-and-conditions) on Wiley Online Library for rules of use; OA articles are governed by the applicable Creative Commons License

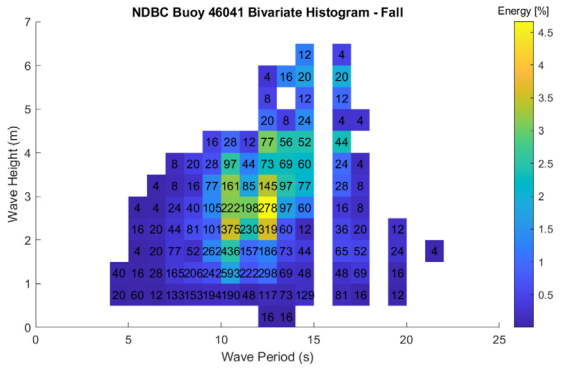


**FIGURE 7** Bivariate histogram of NDBC Station 46041, Fall; bin numbers indicate total occurrences (observed/h) of the sea state over the year; most frequent lies in bin $H_s$ 1.0 to 1.5 m and $T_p$ 10 to 11 s, a value of 593 h/year; colour indicates percent of total energy in the sea state

**TABLE 2** Most occurring $H_s$ and $T_p$ for each season

| Season | $H_s$ [m] | $T_p$ [s] |
|---|---|---|
| Fall | 1.0–1.5 | 10–11 |
| Winter | 2.5–3.0 | 12–13 |
| Spring | 2.0–2.5 | 12–13 |
| Summer | 0.5–1.0 | 7–8 |

of the distribution of sea state parameters. To determine what sea states NDBC Station 46041 operates in, bivariate histograms were made for each of the 4 seasons using historical yearly data from the Station's site page [6]. The data file has a record of hourly samples. The most frequently occurring sea state values were used to develop the irregular sea state as opposed to sea states containing the highest annual energy contribution so that power outputs during analyses represent the power that is most frequently generated at this location. The numbers in the bins on Figure 7 indicate occurrences of the sea state whereas color indicates the respective percentage of annual energy. As an example, Figure 7 is the bivariate histogram for the Fall season with the most occurring sea state taking on $H_s$ and $T_p$ values between 1.0 to 1.5 m and 10 to 11 s, respectively (noted by the 593 in the bin) whereas the sea state with the most energy had bin values of $H_s$ = 2.5 to 3.0 m and $T_p$ = 12 to 13 s. Table 2 summarises the bivariate histogram bins with the most occurring sea states for each season. Note that the absence of data in the 15 s wave period bin is an artifact of the non-linear frequency discretisation utilised by NDBC, which is heavily focused on resolving the high frequency tail of the spectrum rather than the low frequency components. The NDBC post-processing results in no wave periods records between 14.9 and 16.0 s.

## 4.2 | Building the irregular sea state

Many empirical spectra have been developed to characterise sea states. The Bretschneider spectrum was chosen based on the fact that it does not have the hard requirement of needing a fully developed sea and that it is formulated using two parameters, $H_s$ and $w_m$ ($2\pi f_p = \frac{2\pi}{T_p}$) giving a more accurate representation of the true sea state as opposed to one parameter spectra [20, 24]. The span of frequencies, $w$, used to generate the spectrum contain the lowest and highest frequency seen in each season to ensure all observed data from NDBC Station 46041 during 2019 was used in the spectrum calculation. The spectrum is realised using [24]:

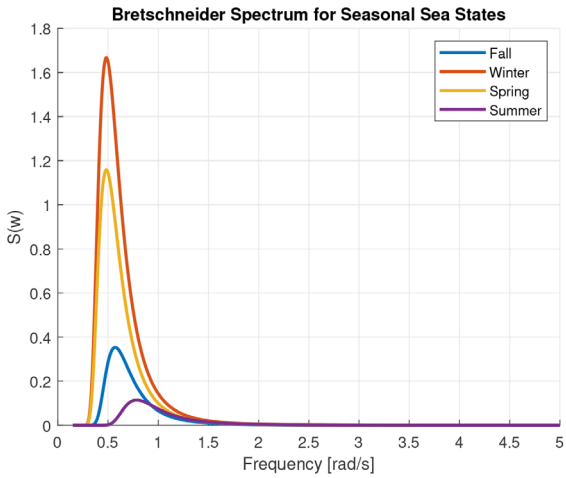


**FIGURE 8** Bretschneider spectrum for NDBC Station 46041 for each season; frequency range to ensure all frequencies from bivariate histograms included

$$S(w) = \frac{5}{16} H_s^2 \frac{w_m^4}{w^5} e^{\frac{-5}{4}\frac{w_m^4}{w^4}} \tag{3}$$

$$w_m = 2\pi f_p = \frac{2\pi}{T_p} \tag{4}$$

Figure 8 shows the Bretschneider spectrum when inputting Equation (3) with the higher range values of Table 2 for each season. The wave surface elevation can then be obtained from:

$$\bar{\eta} = \frac{\sum_{i=1}^{n} \sqrt{2S(w_i)\delta w}}{n} \tag{5}$$

$$\eta = \bar{\eta} + \sum_{i=1}^{n} \sqrt{S(w_i)\delta w} * \cos(wt + \epsilon) \tag{6}$$

where $n$ are the total frequencies considered, $\delta w$ is the frequency step, and $\epsilon$ is a random phase. The wave surface elevation for the Fall season is shown in Figure 9. The seasonal surface elevations developed with these methods will be used in Section 6.

## 5 | SIMPLIFIED PENDULUM EQUATION OF MOTION

In this section we demonstrate the derivation of the equation of motion (EOM) of a horizontal pendulum in only the pitch

17521424, 2021, 14, Downloaded from https://ietresearch.onlinelibrary.wiley.com/doi/10.1049/rpg2.12268 by Battelle Memorial Institute, Wiley Online Library on [29/06/2023]. See the Terms and Conditions (https://onlinelibrary.wiley.com/terms-and-conditions) on Wiley Online Library for rules of use; OA articles are governed by the applicable Creative Commons License

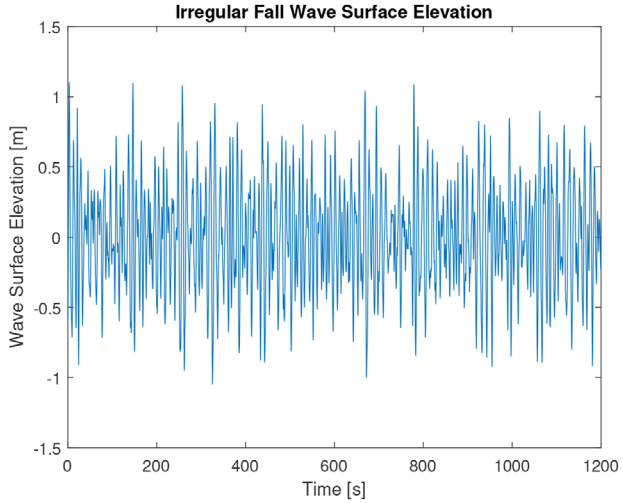


**FIGURE 9** Irregular wave surface elevation NDBC Station 46041, Fall

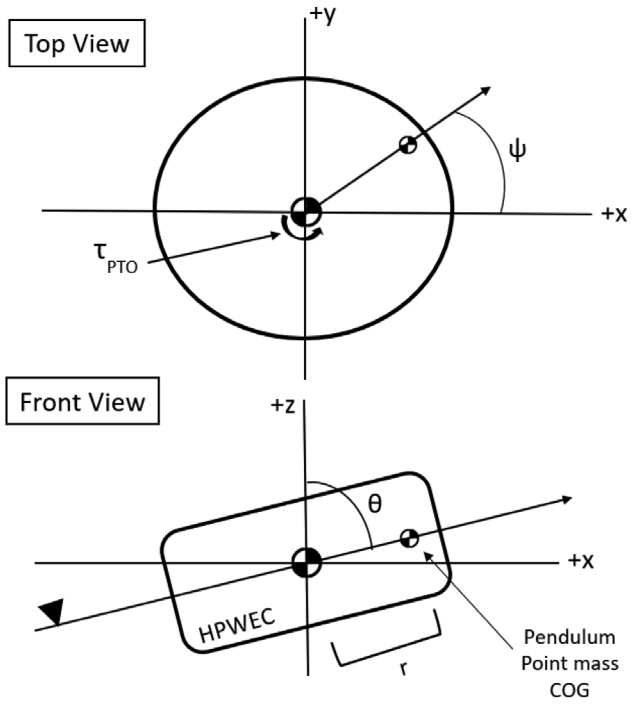


**FIGURE 10** Free body diagram of integrated system to define the Lagrangian and pendulum EOM; $\theta$ denotes pitch, $\psi$ denotes yaw; radius arm length $r$ denotes length between HPWEC COG and pendulum COG; $\tau_{\text{PTO}}$ denotes torque from PTO

degree of freedom (Figure 10), for simplicity of illustration, and demonstration of the principal concept of motion. Formulation of the full equation of motion for all six DOF is complex, and therefore, we solve for the motion in that case numerically using the toolbox WEC-Sim described in Section 6.1. The EOM in pitch is found using Lagrangian mechanics of the difference between the integrated system's total kinetic and potential energy [25]:

$$L = K_{\text{total}} - P_{\text{total}} \tag{7}$$

where $L$ is the Lagrangian, and $K_{\text{total}}$ and $P_{\text{total}}$ are the total kinetic and potential energy, respectively. For the system in pitch, $K_{\text{total}}$ is:

$$K_{\text{total}} = \frac{1}{2} m_{\text{p}} r^2 \dot{\psi}^2 + \frac{1}{2} m_{\text{p}} (r \cos \psi)^2 \dot{\theta}^2 \tag{8}$$

For the system in pitch, $P_{\text{total}}$ is:

$$P_{\text{total}} = g m_p r \cos \psi \cos \theta \tag{9}$$

Combining Equations (8) and (9) into Equation (7) leads to the Lagrangian in pitch as:

$$L = \frac{1}{2} m_{\text{p}} r^2 \dot{\psi}^2 + \frac{1}{2} m_{\text{p}} (r \cos \psi)^2 \dot{\theta}^2 - m_{\text{p}} g r \cos \psi \cos \theta \tag{10}$$

where $m_{\text{p}}$ [kg] is the mass of the pendulum, $g$ is gravitational acceleration (9.81 m/s$^2$), $r$ [m] is the radius arm length, $\theta$ [rad] and $\dot{\theta}$ [rad/s] is the angular position and velocity about the $y$-axis (pitch), $\psi$ [rad] and $\dot{\psi}$ [rad/s] is the angular position and velocity about the $z$-axis (yaw).

The Euler–Lagrange equation is used to obtain the EOM for the angular response of the pendulum:

$$\frac{\mathrm{d}}{\mathrm{d}t}\left(\frac{\partial L}{\partial \dot{\psi}}\right) = \frac{\partial L}{\partial \psi} \tag{11}$$

$$\ddot{\psi} = \frac{m_{\text{p}} g r \sin \psi \cos \theta - m_{\text{p}} r^2 \dot{\theta}^2 \cos \psi \sin \psi}{m_{\text{p}} r^2} \tag{12}$$

where $\ddot{\psi}$ [rad/s$^2$] is the angular acceleration of the pendulum. After applying the non-conservative torque from the damping of the PTO:

$$\ddot{\psi} = \frac{m_{\text{p}} g r \sin \psi \cos \theta - m_{\text{p}} r^2 \dot{\theta}^2 \cos \psi \sin \psi - c\dot{\psi}}{m_{\text{p}} r^2} \tag{13}$$

where $c$ [Nm/(rad/s)] represents PTO damping. Motor viscous damping is neglected as its value is small compared to the PTO damping values considered, explained in detail later in Section 6 numerical modelling. Power from the PTO is then found by:

$$P = \underbrace{\tau_{\text{pto}}}_{c\dot{\psi}} \dot{\psi} = c\dot{\psi}^2 \tag{14}$$

where $\tau_{\text{pto}}$ [Nm] is the torque from the PTO.

The equations for a simple pendulum assume a massless string, the pendulum as a point mass, small oscillations, and no friction, allowing predictions on period and angular frequency to be made based on knowledge of radius arm length [26]. Given that Equation (13) is a second-order nonlinear differential equation for one DOF, the same cannot be said,

17521424, 2021, 14, Downloaded from https://ietresearch.onlinelibrary.wiley.com/doi/10.1049/rpg2.12268 by Battelle Memorial Institute, Wiley Online Library on [29/06/2023]. See the Terms and Conditions (https://onlinelibrary.wiley.com/terms-and-conditions) on Wiley Online Library for rules of use; OA articles are governed by the applicable Creative Commons License

more so with inclusion of all six DOFs. Changing parameters and observing results from numerical simulations are used to draw conclusions about the relationship the design described in Sections 2 and 3 has between power output and varying PTO damping, radius arm length, and pendulum mass values.

## 6 | NUMERICAL MODELLING RESULTS AND DISCUSSIONS

The integrated system was simulated using an iterative process of altering the pendulum radius arm length, pendulum mass, and PTO damping, then checking the effect on power output to examine the effects these parameters have. For clarity, the following definitions are reminded of: radius arm as the distance from the origin of the axis of rotation (centre of HPWEC) to the COG of the pendulum; mass as the mass of the pendulum; and damping as the damping value of the PTO system. Reported power output is the mean power after 20 min WEC-Sim simulations multiplied by 77.4% for total efficiencies as described in Section 3.1. Mass values were based on the size of the HPWEC housing and pendulum within NOAA's hypothetical size constraints (as explained in Section 3.2). This led to a range starting at NOAA's weight limitation of 14 kg to the heaviest weight manufacturing could allow for the size of the pendulum, 100 kg. Damping values were chosen based on preliminary simulations to obtain a rough range of values where the SCOOP base power requirements of 5 W was met and where global maximums in power were observed. This led to a range from 1.5 Nm/(rad/s) to 35 Nm/(rad/s). As mentioned in Section 5, viscous damping is neglected due to its small value compared to the considered damping values. General values of viscous damping are around $1\times10^{-6}$ Nm/(rad/s) [27] whereas the lowest value of PTO damping to be used in simulation is 1.5 Nm/(rad/s). Radius arm values were chosen based on the closest and farthest the pendulum can be to the axis of rotation while staying within the HPWEC cylinder housing.

After describing the software model used to calculate power, results from simulations are then presented. The first parameter investigated is the effect changing the length of the radius arm has on power performance. This reveals a radius arm value that maximises power output for the conditions considered in this case study. This value will be used for the remaining simulations, allowing only a change in two variables instead of three. Patterns in mass and damping values are further analysed in Section 6.3 for each season. Additionally, this section will show which mass and damping values meet the SCOOP power requirements and if they are within imposed weight constraints. Section 6.4 is a brief note on energy storage, followed by a comparison between the pitch motion of the 3 m buoy with and without the addition of the HPWEC, an important consideration to study the effects on the hydrodynamics of the 3 m buoy and what this could mean for accuracy of sensor readings.

### 6.1 | WEC-sim model

To calculate power Equation (14) is used, and as briefly mentioned in Section 5, $\dot{\psi}$ in Equation (14) is found from the six DOF EOM of the system using WEC-Sim (wave energy converter simulator), an open-source code developed by NREL and Sandia National Laboratories (SNL) for simulating WECs using Matlab/Simulink's Simscape Multibody, a multi-body dynamics solver. WEC-Sim allows users to upload custom geometry files, hydrodynamic output files, and setup various PTO and mooring configurations to simulate their design through regular or irregular sea states [28]. The WEC-Sim model used to represent the 3 m buoy and HPWEC modular system are described next.

The SolidWorks files made for each component in the system were saved as stereolithography files to be used in WEC-Sim as visualisation. It was also used to determine COG values at the varying radius arm lengths. MOI values were determined from the assumption of the inertia of a point mass yielding a value equal to the mass times radius arm squared ($m\,r^2$). The hydrodynamic files from Ansys AQWA allow WEC-Sim to know the system's response for certain frequencies that the user chooses to simulate the system through, then uses that information to solve the governing WEC equations of motion in the six Cartesian degrees-of-freedom (DOF).

WEC-Sim's wecSimInputFile.m initialisation script has multiple classes that allow users to define components in their system. Examples of relevant inputs users can make are briefly described. The bodyClass script defines each body (device) in the system and allocates the appropriate hydrodynamic and visual file to it. Users can define the COG (if a non-hydro body), mass, and MOI to the body with their own inputs. The script wavesClass allows users to define the sea state they want to simulate their device in. This was used to import the irregular wave surface elevation for each season derived from Section 4 with a ramp up time of 100 s. The script constraintClass defines the location and orientation of constraints determining how bodies move in relation to one another or to the global coordinate system such as being fixed or moving in all 6-DOF. The script ptoClass defines the PTOs stiffness, damping, location, and orientation. The script mooringClass with lines.txt specific to MoorDyn defines the stiffness properties, locations, and connection points of the mooring system.

The WEC-Sim Simulink Simscape Multibody model describes how devices of the user's system interact with each other and works with the initialisation script to define properties of the blocks in the model. Figure 11 is the Simulink model for the integrated system of this case study. Shown is every component of the integrated system having its own **body** block (3 m buoy, HPWEC cylinder housing, pendulum) defined by their respective COG, MOI, mass, hydrodynamic (if a hydro body) and visual files. The **constraint** blocks describe how the follower (F) is connected to the base (B). For example, the 3 m buoy is connected to the seabed with a 6DOF block meaning it is free to translate or rotate in any of the 6-DOFs with respect to the seabed. The HPWEC cylinder housing has a fixed constraint

17521424, 2021, 14, Downloaded from https://ietresearch.onlinelibrary.wiley.com/doi/10.1049/rpg2.12268 by Battelle Memorial Institute, Wiley Online Library on [29/06/2023]. See the Terms and Conditions (https://onlinelibrary.wiley.com/terms-and-conditions) on Wiley Online Library for rules of use; OA articles are governed by the applicable Creative Commons License

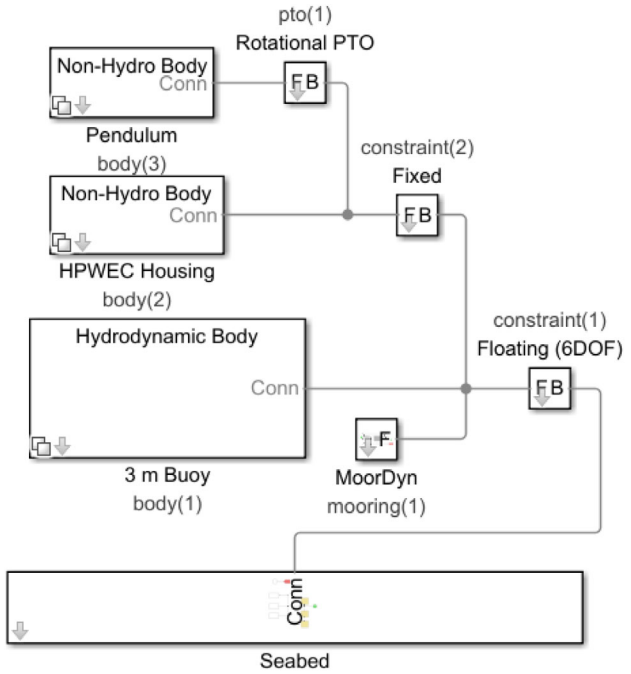


**FIGURE 11** WEC-Sim simulink model of 3 m SCOOP buoy with modular HPWEC; describes how devices of user defined system interact with each other

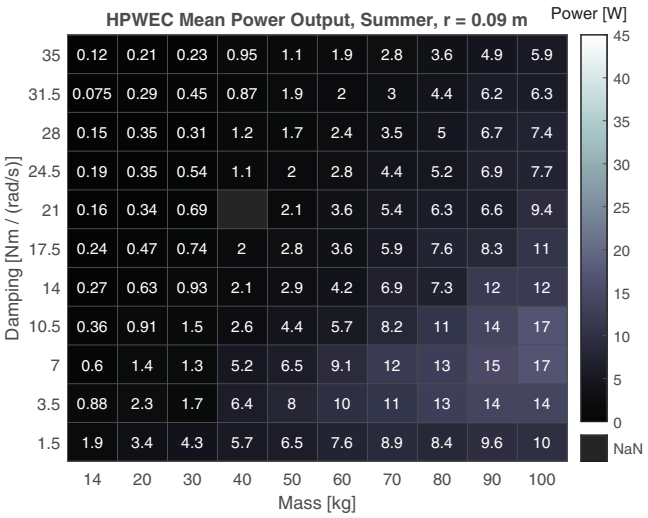


**FIGURE 12** HPWEC Power outputs for the Summer sea state when the radius arm length is 0.09 m; observed lower power results for decrease in length

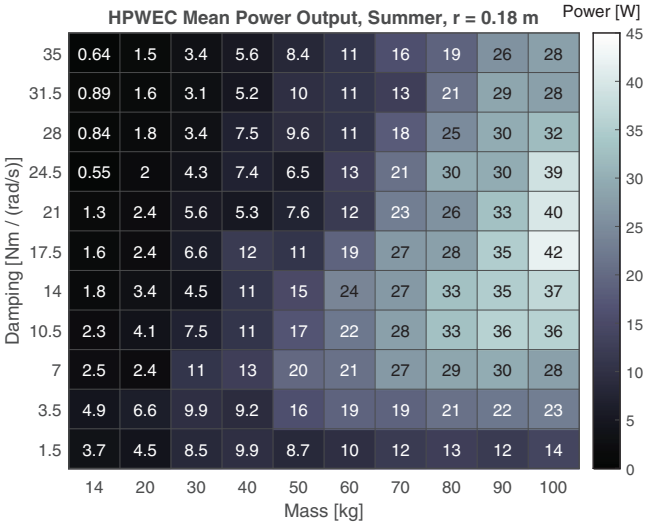


**FIGURE 13** HPWEC Power outputs for the Summer sea state when the radius arm length is 0.18 m; observed higher power results for increase in length

on the 3 m buoy to resemble it being rigidly connected to the buoy, and the pendulum has a rotational PTO which allows it to spin around the HPWEC's central axis defined as location in the ptoClass. Inside the **PTO** block are values for stiffness and damping that the user can change to influence power output and motion response. Finally, the force of the mooring is represented using the MoorDyn library as calculated in Section 2.4. Various radius arm, mass, and damping values were run through this model and the initialisation script in calculating and observing the effects on power and motion response, described next.

## 6.2 | Radius arm choice

To study the effects radius arm length have on power output, the value is changed between lengths of 0.09 to 0.18 m for the Summer sea state. Summer was chosen as it has the lowest energy sea state and is expected to produce the lowest power output out of all seasons. Results are shown in Figures 12 and 13 for $r = 0.09$ m and $r = 0.18$ m, respectively.

The trend of increase in power was consistent with increase in radius arm length and was evident across the Fall, Spring, and Winter sea states. To simplify the remaining simulations, the longest radius arm allowed within the size of the HPWEC, 0.18 m, is used for the remaining simulations as it allowed for the highest production of power. It is important to note that the pendulum's ever changing COG has a direct effect on the hydrodynamics of the 3 m buoy in its response to the sea state. Drastic behavior of this is evident by the "NaN" (not a number) value in Figure 12 caused by singularities encountered when solving the governing equations. This could be a result of nonlinear hydrodynamics not included in simulations and is an important topic for future work.

## 6.3 | Mass and damping effect on seasonal power outputs

Now that the radius arm value that yields the highest power output across all sea states has been determined this variable can be fixed, simplifying the remaining simulations to explore the effect of damping and mass values on power output for all seasons. This is shown in Figures 14–17 for Fall, Winter, Spring, and Summer seasons respectively.

17521424, 2021, 14, Downloaded from https://ietresearch.onlinelibrary.wiley.com/doi/10.1049/rpg2.12268 by Battelle Memorial Institute, Wiley Online Library on [29/06/2023]. See the Terms and Conditions (https://onlinelibrary.wiley.com/terms-and-conditions) on Wiley Online Library for rules of use; OA articles are governed by the applicable Creative Commons License

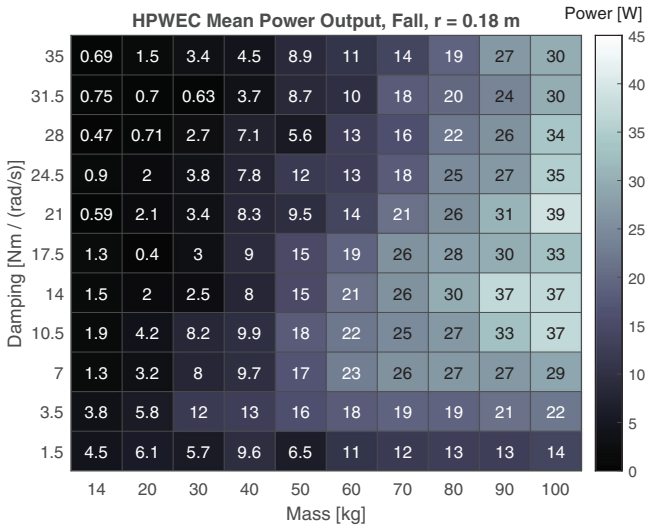


**FIGURE 14** HPWEC Power outputs for the Fall irregular sea state; 5 W base requirement met for masses 20 kg and over and varying damping ranges

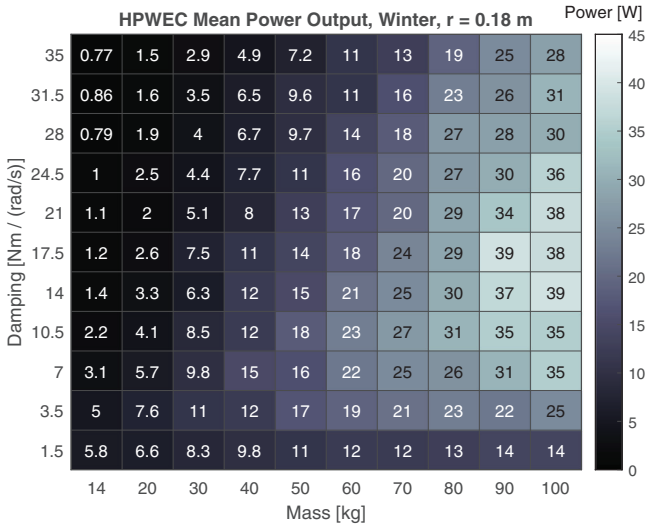


**FIGURE 15** HPWEC Power outputs for the Winter irregular sea state; 5 W base requirement met for masses 14 kg and over and varying damping ranges

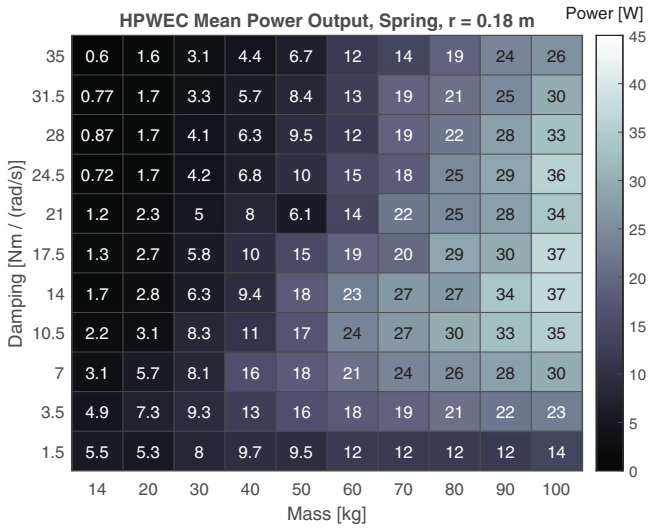


**FIGURE 16** HPWEC Power outputs for the Spring irregular sea state; 5 W base requirement met for masses 14 kg and over and varying damping ranges

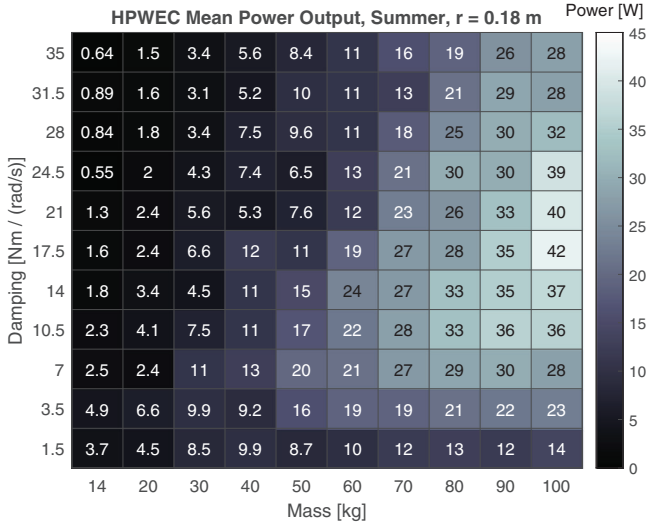


**FIGURE 17** HPWEC Power outputs for the Summer irregular sea state; 5 W base requirement met for masses 20 kg and over and varying damping ranges

Power outputs consistently increased with higher pendulum mass values and a constant damping value with the exception of certain damping values at 50 kg. Power maximised for certain ranges of damping with a constant mass, decreasing once the damping was too high as the direct negative impact it had on speed ultimately lowered the power. These two observations can lead to general ranges of damping desired for mass ranges. For example, during the Fall season (Figure 14) power was generally maximised for a damping range of 10.5 to 21.0 Nm/(rad/s) for heavier masses (50 kg and above) and 1.5 to 10.5 Nm/(rad/s) for lighter masses (50 kg and below). Power outputs were seen to decrease when below or above these damping ranges for the corresponding mass range, again, due to the dependent relationship of speed and damping and their trade-off on power output. Interestingly, while a power increase was evident with mass increase, the magnitude of power did not significantly change throughout the four seasons. For example, the power values in the lowest energy sea state, Summer, are similar to that of the highest energy sea state, Winter. This aligns well with [19] where tank tests were conducted on a pendulum WEC, concluding that larger waves resulted in higher mean power outputs only a portion of the time. This is true when observing Figures 15 and 17 where Winter generally outperforms Summer, but not significantly in magnitude for each mass and damping combination. Although seasonal power trends are typically common among WEC devices, the absence of outstanding

17521424, 2021, 14, Downloaded from https://ietresearch.onlinelibrary.wiley.com/doi/10.1049/rpg2.12268 by Battelle Memorial Institute, Wiley Online Library on [29/06/2023]. See the Terms and Conditions (https://onlinelibrary.wiley.com/terms-and-conditions) on Wiley Online Library for rules of use; OA articles are governed by the applicable Creative Commons License

variability could prove to be an advantage to users when choosing sensors to operate within their rated power conditions.

Finally, it is evident power outputs in every season other than Winter and Spring do not produce the base SCOOP power requirement of 5 W within the presently-assumed mass constraint of 14 kg. Therefore the minimum mass value to meet the base power requirement yearly is examined. A minimum mass of 20 kg is capable of meeting the base requirement of 5 W for all seasons of the year. The damping value may change per season to capture more energy or stay at 3.5 Nm/(rad/s) to meet the base requirement.

Another important observation is the effect of inertia on the system's power performance. This study showed that an increase in inertia from heavier masses led to a higher power output, however in this particular case study the problem was restricted in ways such as the assumption of a point mass for MOI and limitations in mass and radius length values due to NOAA size constraints and physical manufacturing capabilities. It is key to continue further simulations in the future that have a broader focus with less restrictions on using differing pendulum designs and MOIs to better understand the inertia effect on the dynamics of the integrated system and its response to the sea state as well as the effects on power output.

## 6.4 | Energy storage

The current power system for the SCOOP is a 10.8 V 1.34 kWh battery [29]. The range of energy ripple produced by the HPWEC was determined by integrating the power time series after removing the average power, representing the energy leftover to be stored. To establish the upper storage capacity needed, the time series was taken from the season that produced the highest power using the earlier defined yearly mass value of 20 kg. This corresponds to the Winter season with a a 3.5 Nm/(rad/s) damping value to produce the highest power. The power, power ripple, and energy ripple time series of this scenario is shown in Figure 18. The battery capacity needed to meet the energy range is:

$$\text{Batt}_{\text{cap}} = \frac{E_{\max}}{3600\frac{\text{s}}{\text{hr}} * V} \tag{15}$$

where $\text{Batt}_{\text{cap}}$ [Ah] is the capacity of the battery, $E_{\max}$ [J] is the maximum energy to be stored, and $V$ [V] is the voltage of the SCOOP power system (10.8 V). This results in a battery capacity of 0.03 Ah. To get units of Watt-hours, the battery capacity is multiplied by the voltage of the SCOOP power system, yielding a value of roughly 0.5 Wh. The existing system of 1.34 kWh is sufficient then to buffer the output from the HPWEC. It is also noted that while the yearly mass value of 20 kg does not produce the peak power requirement of 16.5 W for any season, the accumulation from energy storage would allow supply of peak power when needed for periodic data transmission bursts.

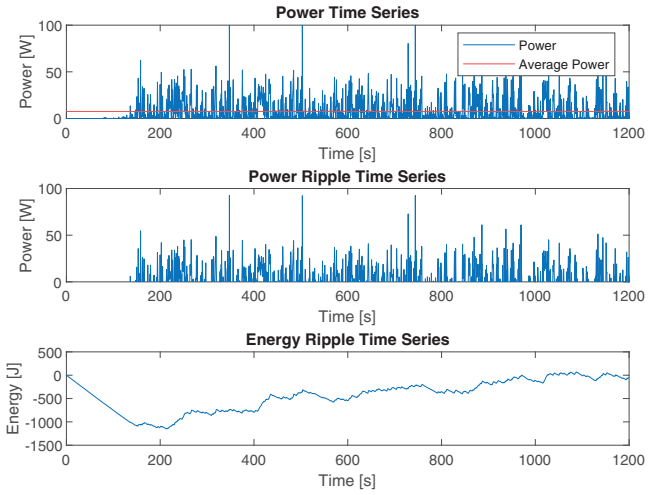


**FIGURE 18** Power, and power and energy ripple time series of HPWEC in Winter sea state with a pendulum mass of 20 kg and damping 3.5 Nm/(rad/s); 0.5 Wh energy storage capacity needed for HPWEC, SCOOP 1.34 kWh sufficient to buffer

**TABLE 3** RMSE values for Winter and Summer sea states with 20 kg and 100 kg pendulum masses

| Season | Mass [kg] | Damping [Nm/(rad/s)] | RMSE |
|---|---|---|---|
| Summer | 20 | 3.5 | 0.2828 |
| | 100 | 17.5 | 0.3190 |
| Winter | 20 | 3.5 | 0.3248 |
| | 100 | 14 | 0.3485 |

## 6.5 | Comparing pitch motion between 3 m buoy with and without the HPWEC

With the addition of the HPWEC on the 3 m buoy, the response to oncoming waves will differ from without the HPWEC. As a result, the SCOOP payload on the buoy will have different sensor readings of environmental conditions, possibly leading to false representations of the true conditions. To study the effect of the HPWEC on the 3 m buoys response to sea states, the root mean square error (RMSE) values for the pitch motion of the 3 m buoy with and without the HPWEC are shown in Table 3 for the lowest and largest sea states (Summer and Winter). Additionally, Table 3 shows the difference in RMSE when the mass of the pendulum is 20 kg versus 100 kg. Each scenario used the damping value that maximised power from the results in Section 6.3 for Summer and Winter, and a radius arm of 0.18 m. Figure 19, Figures 20–22 depict the time series of pitch motion for an arbitrary time range for these cases.

As expected, the pitch response of the 3 m buoy has changed when the HPWEC is fixed onto its platform . The effect is slightly more dramatic in the Winter versus Summer seen by the increase in RMSE values compared between the two sea states due to the more energetic sea state present in Winter. The use of a heavier mass also results in a larger RMSE due

17521424, 2021, 14, Downloaded from https://ietresearch.onlinelibrary.wiley.com/doi/10.1049/rpg2.12268 by Battelle Memorial Institute, Wiley Online Library on [29/06/2023]. See the Terms and Conditions (https://onlinelibrary.wiley.com/terms-and-conditions) on Wiley Online Library for rules of use; OA articles are governed by the applicable Creative Commons License

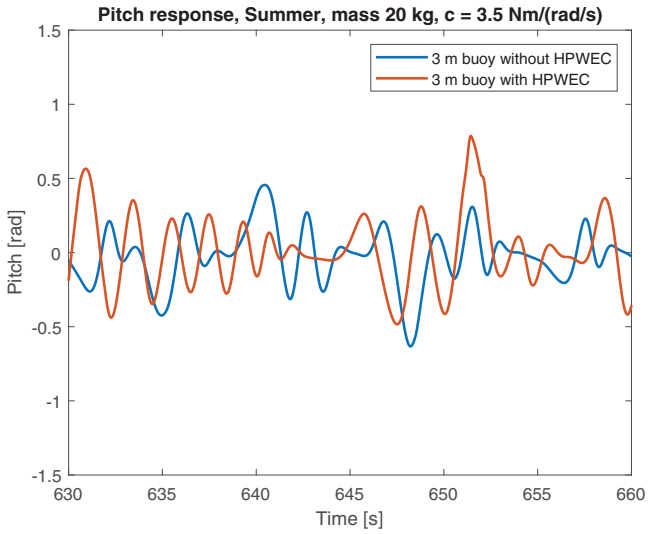


**FIGURE 19** Pitch motion of 3 m buoy with and without the HPWEC for the Summer sea state with a pendulum mass of 20 kg, damping of 3.5 Nm/(rad/s), and 0.18 m radius arm; RMSE = 0.2828 over entire simulation time; arbitrary time range shown

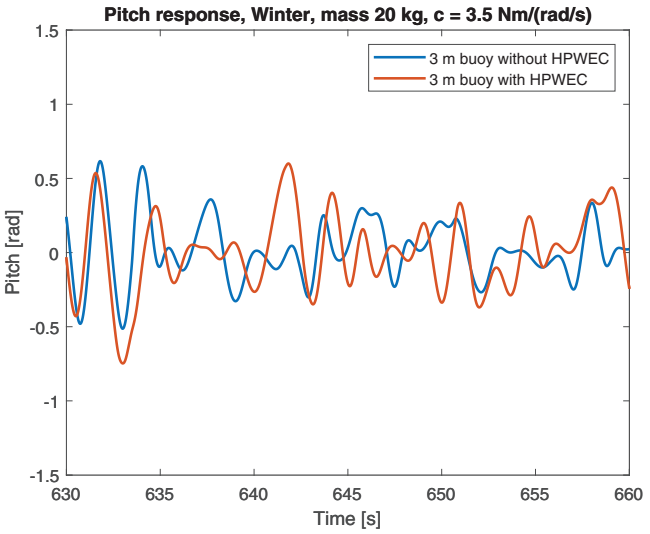


**FIGURE 21** Pitch motion of 3 m buoy with and without the HPWEC for the Winter sea state with a pendulum mass of 20 kg, damping of 3.5 Nm/(rad/s), and 0.18 m radius arm; RMSE = 0.3248 over entire simulation time; arbitrary time range shown

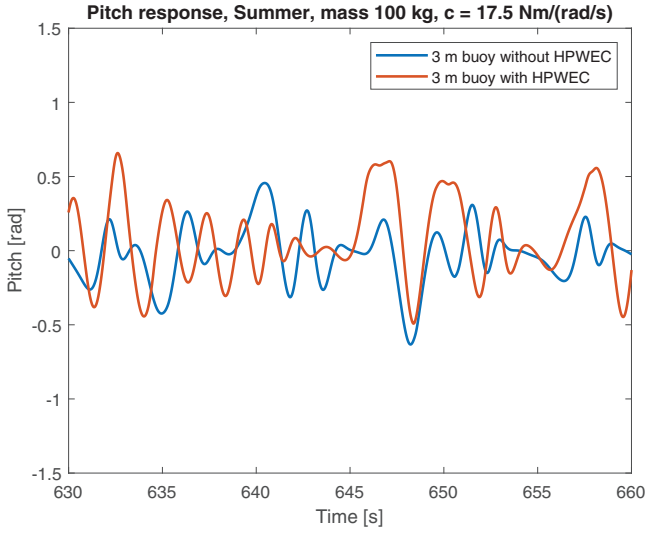


**FIGURE 20** Pitch motion of 3 m buoy with and without the HPWEC for the Summer sea state with a pendulum mass of 100 kg, damping of 17.5 Nm/(rad/s), and 0.18 m radius arm; RMSE = 0.3190 over entire simulation time; arbitrary time range shown

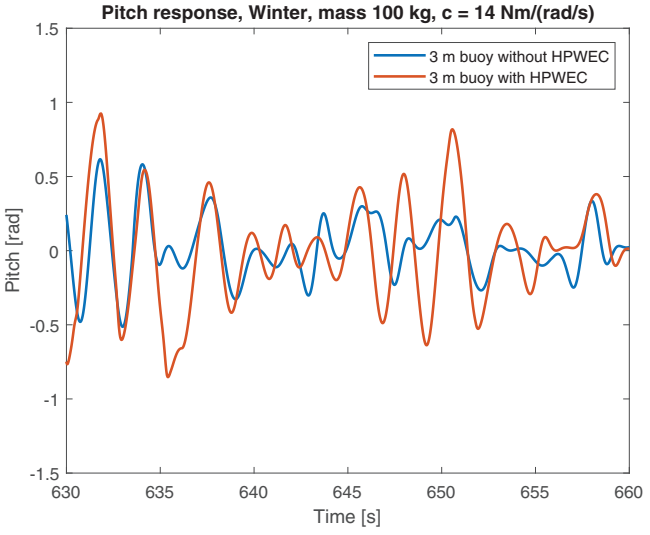


**FIGURE 22** Pitch motion of 3 m buoy with and without the HPWEC for the Winter sea state with a pendulum mass of 100 kg, damping of 14 Nm/(rad/s), and 0.18 m radius arm; RMSE = 0.3485 over entire simulation time; arbitrary time range shown

to the different COG and its influence as it changes location according to the pendulums motion, thus changing the COG of the entire integrated system. Future work will include more detailed analysis on the impact the HPWEC has on the buoy and accuracy of sensor measurements.

## 7 | CONCLUSION

MRE as the main power source for marine applications has received positive feedback by users in this sector [2]. Compared to solar, battery, wind, or diesel generators, it has been identified as an advantageous alternative [1, 3]. To further these studies, this paper investigated the feasibility of a specific WEC design powering one of these applications. The HPWEC design was chosen for its robustness and was applied to NDBC SCOOP weather buoys as a low bound for determining power requirements that this design can meet. This paper analysed the effects pendulum mass, radius arm length, and damping of the PTO had on the seasonal power output of the HPWEC. Increases in mass and radius arm equated to higher power output, a consistent trend seen for every season, while ranges of damping that maximised power were dependent on the mass value and sea state.

17521424, 2021, 14, Downloaded from https://ietresearch.onlinelibrary.wiley.com/doi/10.1049/rpg2.12268 by Battelle Memorial Institute, Wiley Online Library on [29/06/2023]. See the Terms and Conditions (https://onlinelibrary.wiley.com/terms-and-conditions) on Wiley Online Library for rules of use; OA articles are governed by the applicable Creative Commons License

The most notable finding related to power performance was that in order to meet the SCOOP base power requirement of 5 W for the entire year, the mass of the pendulum (and therefore the modular HPWEC) was over the considered mass constraint of 14 kg, calling for a minimum value of 20 kg. Although the 20 kg pendulum mass is required to meet the base SCOOP power of 5 W, another scenario to consider would be using both the HPWEC and solar panels already installed on the 3 m SCOOP buoys to supply power to the payload. This way, solar could be the main power source in the lower sea state seasons with the additional production by the HPWEC. The HPWEC could then be the main source in the higher sea state seasons. This would effectively add supplementary power to the current solar panel power source of the 3 m SCOOP buoy while maintaining the possibility for longer deployments and remote area operation. With a combined system, the weight of the HPWEC could decrease as it is not the sole supplier of power, thus meeting the mass constraint.

It was confirmed that the addition of the HPWEC on the 3 m buoy changed the buoy's motion when compared to operation without it as a result of the changing COG associated with the rotational movement of the pendulum. The RMSE between the pitch response of the 3 m buoy with and without the HPWEC showed a clear change in buoy behaviour, increasing with larger sea states and mass. This will have effects on the sensor data output and is important to further study to ensure the addition of a modular device such as the HPWEC still permits the buoy to record accurate data readings. Also, the possible nonlinear hydrodynamic behaviour of the 3 m buoy caused by the changing COG is another feature to study as this can affect the power output and buoy motion as well. Furthermore, the findings in this paper hold for a system with a certain range of considered values for one pendulum design due to restrictions on size and weight. To better understand pendulum influence and the associated inertial properties on the 3 m buoys hydrodynamic response, a variety of designs should be studied. Future work will focus on a better understanding of this behavior leading to more accurate results of power output and buoy motion, possibly reducing or increasing the range of masses and size constraints considered. This will further aid understanding the feasibility of using HPWECs to realise the benefits they may provide.

## ACKNOWLEDGMENTS

This research was conducted with assistance from researchers from Oregon State University's Civil and Electrical and Computer Engineering Departments.

This research was supported in part by an appointment with Marine and Hydrokinetic Graduate Student Research Program sponsored by the U.S. Department of Energy (DOE), Office of Energy Efficiency and Renewable Energy, and Water Power Technologies Office. This program is administered by the Oak Ridge Institute for Science and Education (ORISE) for the DOE. ORISE is managed by ORAU under DOE contract number DESC0014664. All opinions expressed in this paper are the author's and do not necessarily reflect the policies and views of DOE, ORAU, or ORISE.

This work was authored in part by the Pacific Northwest National Laboratory, operated by Battelle Memorial Institute for the U.S. Department of Energy (DOE) under Contract No. DE-AC05-76RL01830. Funding provided by the U.S. Department of Energy Office of Energy Efficiency and Renewable Energy Water Power Technologies Office. The views expressed herein do not necessarily represent the views of the DOE or the U.S. Government. The U.S. Government retains and the publisher, by accepting the article for publication, acknowledges that the U.S. Government retains a nonexclusive, paid-up, irrevocable, worldwide license to publish or reproduce the published form of this work, or allow others to do so, for U.S. Government purposes.

## ORCID

*Chris Dizon* https://orcid.org/0000-0003-2063-6981

## REFERENCES

1. LiVecchi, A. et al.: Powering the Blue Economy; Exploring Opportunities for Marine Renewable Energy in Maritime Markets. U.S. Department of Energy, Office of Energy Efficiency and Renewable Energy, Washington, D.C. (2019)
2. Green, R. et al.: Enabling power at sea: Opportunities for expanded ocean observations through marine renewable energy integration. In: OCEANS 2019 MTS/IEEE SEATTLE, pp. 1–7. IEEE, Piscataway, NJ (2019)
3. Cavagnaro, R.J., et al.: Powering the blue economy: Progress exploring marine renewable energy integration with ocean observations. Mar. Technol. Soc. J. 54(6), 114–125 (2020)
4. Koca, K. et al.: Recent advances in the development of wave energy converters. Paper presented at the 10th European wave and tidal energy conference, Aalborg, 2–5 Sept 2013
5. WPTO Announces $4.4 Million for Phase I Small Business Innovation Projects. https://www.energy.gov/eere/water/articles/wpto-announces-44-million-phase-i-small-business-innovation-projects. Accessed June 14, 2021
6. Station 46041 (LLNR 733) - CAPE ELIZABETH- 45NM NW of Aberdeen, WA. https://www.ndbc.noaa.gov/station_page.php?station=46041. Accessed February 7, 2021
7. Lehmann, M., et al.: Ocean wave energy in the United States: Current status and future perspectives. Renewable Sustainable Energy Rev. 74, 1300–1313 (2017)
8. Lenee-Bluhm, P., Paasch, R., Özkan-Haller, H.T.: Characterizing the wave energy resource of the US Pacific Northwest. Renewable Energy 36(8), 2106–2119 (2011)
9. 3 Metre Met Ocean Buoy. https://axystechnologies.com/wp-content/uploads/2014/11/3-Metre-Buoy.pdf#:~:text=The%20expected%20service%20life%20of%20the%203%20metre,buoys%20have%20never%20been%20retired%20due%20to%20corrosion. Accessed February 7, 2021
10. IEC 61701: Photovoltaic (PV) modules – Salt mist corrosion testing', (2020)
11. Bouchard, R.H. et al.: Field Evaluation of the Wave Module for NDBC's New Self-Contained Ocean Observing Payload (SCOOP) on Modified NDBC Hulls. http://www.waveworkshop.org/15thWaves/Presentations/A2.pdf. Accessed February 7, 2021
12. Craig Kohler, P.E., LeBlanc, L., Elliott, J.: SCOOP - NDBC's new ocean observing system. In: OCEANS 2015 - MTS/IEEE Washington, pp. 1–5. IEEE, Piscataway, NJ (2015)
13. Dassault Systèmes: SolidWorks 2020 (Version 2020) [Computer Program]. https://www.solidworks.com/. Accessed February 2, 2021

17521424, 2021, 14, Downloaded from https://ietresearch.onlinelibrary.wiley.com/doi/10.1049/rpg2.12268 by Battelle Memorial Institute, Wiley Online Library on [29/06/2023]. See the Terms and Conditions (https://onlinelibrary.wiley.com/terms-and-conditions) on Wiley Online Library for rules of use; OA articles are governed by the applicable Creative Commons License

14. Ansys: Ansys Aqwa: Hydrodynamics Simulation & Diffraction Analysis (Version 19.1) [Computer Software]. https://www.ansys.com/products/structures/ansys-aqwa. Accessed February 2, 2021
15. Moored Buoy Program. https://www.ndbc.noaa.gov/mooredbuoy.shtml. Accessed February 7, 2021
16. Meindl, A.: GUIDE TO MOORED BUOYS AND OTHER OCEAN DATA ACQUISITION SYSTEMS, Data Buoy Co-operation Panel Technical Document No. 8. https://repository.oceanbestpractices.org/bitstream/handle/11329/81/DBCP-08-Guide-Moored-Buoys.pdf?sequence=1&isAllowed=y. Accessed February 7, 2021
17. MoorDyn User's Guide. http://www.matt-hall.ca/files/MoorDyn-Users-Guide-2017-08-16.pdf. Accessed May 24, 2021
18. Chain properties. https://documentation.dsaocean.com/tutorials/Tutorials/PDS-AAR.html. Accessed February 7, 2021
19. Dinovitzer, A. et al.: The mooring selection guide (MSG) software. In: OCEANS '97. MTS/IEEE Conference Proceedings, pp. 126–133. IEEE, Piscataway, NJ (1997)
20. Boren, B.: On the Modeling and Control of Horizontal Pendulum Wave Energy Converters. Master's Thesis, Oregon State University (2013)
21. Yurchenko, D., Alevras, P.: Parametric pendulum based wave energy converter. Mech. Syst. Sig. Process. 99(1), 504–515 (2018)
22. Mongird, K. et al.: Energy Storage Technology and Cost Characterization Report. https://www.energy.gov/sites/prod/files/2019/07/f65/Storage%20Cost%20and%20Performance%20Characterization%20Report_Final.pdf. Accessed May 24, 2021
23. Wave Energy Harvesting to Power Ocean Buoys. https://www.sbir.gov/sbirsearch/detail/1834913. Accessed May 25, 2021
24. Goda, Y.: Random Seas and Design of Maritime Structures. vol. 33, World Scientific Publishing, Singapore (2010)
25. Morin, D.: The Lagrangian Method. https://scholar.harvard.edu/files/david-morin/files/cmchap6.pdf. Accessed February 12, 2021
26. Mohazzabi, P., Shankar, S.: Damping of a simple pendulum due to drag on its string. J. Appl. Math. Phys. 5, 122–130 (2017)
27. Kecskés, I., Burkus, E., Odry, P.: Gear efficiency modeling in a simulation model of a DC gearmotor. In: 2018 IEEE 18th International Symposium on Computational Intelligence and Informatics (CINTI), pp. 000065–000070. IEEE, Piscataway, NJ (2018)
28. Yi-Hsiang, Y. et al.: WEC-Sim. https://doi.org/10.5281/zenodo.3924764. Accessed February 12, 2021
29. Elliot, J., Riley, R.: NDBC's SCOOP Update: Oceans in Action. https://www.mset.org/resources/documents/presentations/OIA2014/11_NDBC_New_Ocean_Observing_Platfom-R_Riley_and_J_Elliot.pdf. Accessed February 7, 2021

**How to cite this article:** Dizon, C., et al. Modular horizontal pendulum wave energy converter: Exploring feasibility to power ocean observation applications in the U.S. pacific northwest. IET Renew. Power Gener. 15:3354–3367 (2021). https://doi.org/10.1049/rpg2.12268

17521424, 2021, 14, Downloaded from https://ietresearch.onlinelibrary.wiley.com/doi/10.1049/rpg2.12268 by Battelle Memorial Institute, Wiley Online Library on [29/06/2023]. See the Terms and Conditions (https://onlinelibrary.wiley.com/terms-and-conditions) on Wiley Online Library for rules of use; OA articles are governed by the applicable Creative Commons License